Failure maps to assess bearing performances of glass composite laminates

Journal:	*Polymer Composites*
Manuscript ID	Draft
Wiley - Manuscript type:	Research Article
Date Submitted by the Author:	n/a
Complete List of Authors:	Calabrese, Luigi; Universita degli Studi di Messina Fiore, Vincenzo; University of Palermo, Dipartimento di Ingegneria civile, ambientale, aerospaziale, dei materialia Scalici, Tommaso; University of Palermo, Department of "Ingegneria Civile, Ambientale, Aerospaziale, dei Materiali Bruzzaniti, Paolo; Universita degli Studi di Messina Valenza, Antonino; University of Palermo,
Keywords:	failure, mechanical properties, composites, strength

Failure maps to assess bearing performances of glass composite laminates

L. Calabrese[1], V. Fiore[2*], T. Scalici[2], P. Bruzzaniti[1], A. Valenza[2]

[1]Department of Electronic Engineering, Industrial Chemistry and Engineering, University of Messina

Contrada Di Dio (Sant'Agata), 98166 Messina, Italy

[2]Department of "Ingegneria Civile, Ambientale, Aerospaziale, dei Materiali", University of Palermo

Viale delle Scienze, Edificio 6, 90128 Palermo, Italy

Email: vincenzo.fiore@unipa.it

*Corresponding Author

Abstract

Aim of the present paper is the assessment of the bearing mechanical performances of pin-loaded glass laminates as function of their geometrical configuration. To this concern, 32 specimens having different hole diameter (D), laminate width (W) and hole center to laminate free edge distance (E) have been tested under bearing conditions. The maximum bearing stress and the stress-displacement curves were analyzed as function both of hole to laminate free edge distance E and hole diameter D. Moreover, an experimental 2d failure map was created by placing the experimental results (i.e., the kind of failure mechanism occurred for each geometrical configuration) in the plane E/D versus W/D ratios. In order to identify a simplified methodology able to design mechanically fastened joints in an easy and effective way, a simplified theoretical failure map on E/D and W/D axes was proposed. The theoretical model showed a good matching with the experimental results validating the proposed approach. In particular, the proposed simplified failure map highlighted that, for woven glass fibre composite laminates fastened joints should have E/D and W/D ratios higher than 1.6 and 2.1, respectively, in order to stimulate a progressive bearing failure mechanism and achieve the full laminate strength. Finally, another goal of the present paper was to assess failure mechanisms evolution by drawing a 3D plot (i.e., at varying E/D and W/D geometrical ratios) of the failure index (FI) evaluated for each failure mechanism according to the maximum stress criterion.

Keywords: Bearing, failure modes, mechanical joints, glass fibre, failure map

1 Introduction

Nowadays, composite structures are widely used instead of conventional metal materials in several engineering fields thanks to their features such as low density, high mechanical performances, good corrosion resistance and so on. For instance, while the use of fibre-reinforced polymer (FRP) was limited to aerospace applications until early 1990s, by the mid-1990s this class of materials begins to be used also for nautical, civil and automotive ones.

Whatever is the application area, the use of monolithic structures is extremely rare or limited to very specific application so that there is always the necessity to join composite components to other composites or metallic parts [1–5] in order to produce the whole structure. Normally, the parts made of composites are realized by hand lay-up, vacuum bagging or other manufacturing technique and then they are joined with metal ones through a structural adhesive, a mechanical connection or a combination of these last [6]. The mechanical or adhesive connections can be considered as the weakest part within a construction system since often the structure collapse originated from them [7].

It is worth noting that despite the use of adhesive bonded joints allow to avoid delamination phenomena due to the absence of holes, to reduce the weight structure, to prevent degradation phenomena due to galvanic corrosion, on the other hand this technology cannot be used in structures which require subsequent disassembly for maintenance, inspection and repair. Furthermore, mechanical connections such as bolting, riveting and self-piercing riveting are easier to realize and allow to realize structures able to sustain higher loads. Due to the common use of mechanical connection in composite or hybrid structures, the exploitation of full potential of composite materials in the design of mechanical joints is required. To this aim, a deep understanding of failure mechanisms and mechanical behaviours of joints is strictly necessary [8]. As widely known, pin-loaded composites laminates can exhibit four different failure mechanisms: i.e., bearing, net-tension, shear out and cleavage [1]. Among them, bearing is the only not

catastrophic mechanism: i.e., it is characterized by a progressive and gradual compressive collapse of composite in contact with pin, thus providing an effective warning before the complete failure of the mechanical joint. On the other hand, both net tension [9,10] and shear out [11,12] are sudden and catastrophic mechanisms, thus leading to joints fractures at very low load and displacement values. Being a mixed mode between net-tension and shear out, cleavage is also a low-strength joint failure, due to a combination of both tension and shear stresses [13].

The maximum strength of mechanically fastened joints in composite structures, strictly related to the pin-loaded composite failure mode, depends on many factors such as joint geometry, fibre orientation, and stacking sequence [14–16]. In particular, as the failure of joints is remarkably affected by the geometric configuration of the composite substrates, the influence on the failure of joints of geometrical parameters such as hole diameter, composite width and thickness, distance between the hole and the composite free edge has been widely discussed by several researchers [14,17–20]. In most papers concerning composite mechanical joints the interactions between hole diameter (D) and composite dimensions such as width (W) and distance from hole centre to composite free edge (E), resulting in W/D and E/D ratios, are considered the main parameters for joint design. In this context, designers are required to obtain the optimum E/D and W/D ratios to get the bearing mode, thus achieving the laminate full strength.

A useful design approach can be the identification of methodologies to predict the damage strength limit and failure mode of fastened mechanical composite joints. In fact, an important issue is that all aspects of the joining design are well understood. In this concern, reliable and effective assessment methods are required in order to minimize the weights of the joined structure as well as the product and in service life costs. In the literature, very accurate models to predict performances and failure modalities of bolted composite structures are mainly based on the implementation of finite elements numerical models (FEM) [21–25]. Such models, although they may predict the mechanical behaviour of the structure, require a well structured parameterization of the model as well as long

calculation times. In order to avoid these penalties, theoretical or empirical approach could be an effective alternative in the joining design. Camanho and Lambert [26] proposed a procedure to forecast the final failure and damage mode of mechanically fastened joints in composite laminates by using semi-analytical or numerical methods. Both analytical and numerical methods of stress analysis can be applied to predict failure evaluating joints parameters as clearance, friction and geometry [27] [28].

However, an important still pending issue in engineering joining, that require further investigation, is to identify a simplified methodology able to design mechanically fastened joints in a fast and effective way. In this concern, pin-loaded glass laminates have been tested under bearing conditions at varying W/D and E/D ratios. The maximum bearing stress and the stress-displacement curves were analyzed as function of both hole to laminate free edge distance E and hole diameter D.

Moreover, an experimental 2D failure map was created by placing the experimental results (i.e., the kind of failure mechanism occurred for each geometrical configuration) in the plane E/D versus W/D ratios. By using a simplified theoretical model, having a very good match with the experimental data, the E/D versus W/D plane was clearly divided into three regions related to the typical failure mechanisms of mechanically-fastened joints. Finally, it were accurately captured 3D shape information for the evaluation of the failure mechanisms by drawing a 3D plot (i.e., at varying E/D and W/D geometrical ratios) of the failure index (FI) evaluated for each failure mechanism according to the maximum stress criterion.

The proposed simplified approach can be effectively used to generate design failure map for composite bolted joints containing open holes which can be used to have a topological image of the fracture mechanisms related with joint geometries, thus allowing designer to orient intuitive and reliable joining solutions.

2 Material and methods

A GFRP composite panel with dimension of 350 x 350 mm^2 and nominal thickness of 3 mm was produced by vacuum assisted resin infusion, cured at 25 °C for 24 hours and post-cured at 50 °C for 8 hours. An epoxy resin SX8 EVO (Mates Italiana s.r.l., Italy) and 16 layers of plain weave woven glass fabrics with nominal areal weight of 200 g/m^2 (Mike Compositi, Italy) were used as matrix and reinforcement, respectively.

With the aid of a band saw, prismatic samples with length of 150 mm were cut from the above panel. A single hole was carried out on each specimen by using at first a undersized drilling bits and then a mill tool in order to achieve the desired hole diameter avoiding edge defects. Table 1 details the geometric parameters of all composite samples used for bearing tests. In particular the hole diameter D and the distance between the hole centre and the laminate free edge, E, were varied in the ranges 4-10 mm, 4-19 mm, respectively. In this way, it can possible to evaluate the effect of W/D and E/D geometrical ratios both on the mechanical behaviour and on the failure mechanisms of pin-loaded GFRP laminates.

The mechanical bearing tests were carried out, according to ASTM D5961/D standard (procedure A), using a universal testing machine Z250 (Zwick-Roell, Germany), equipped with a 250 kN load cell. Each test was performed in displacement control mode by setting the displacement equal to 0.5 mm/min. Geometry of composite samples and the scheme of joint configuration used for the bearing test are shown in Figure 1.

For each bearing test, the specimen was fastened by using a bolt to a specially designed steel plate thus reducing its rotation. In particular, the stainless steel insert was positioned in the hole, afterward Bearing tests were performed applying a tensile load P on the plate, in parallel direction to the symmetry plane of the plate and composite sample in order to avoid unwanted moments and rotations.

3 Results and discussion

As widely known, a pin-loaded composite laminate can exhibit four different failure modes: namely shear out, net tension, cleavage and bearing. The failure mode experienced is function both of the material properties (stacking sequence, kind of fibre etc.) and of the geometrical configuration. In particular, it is possible to modify the failure mode for a given composite laminates by varying one or more of the following geometrical parameters: laminate thickness t, hole diameter D, laminate width W and distance between the hole centre and the laminate free edge E.

Except for the cleavage mixed mode, it is possible calculate the stress values for each failure mode by a simplified theoretical approach [11,18,29]. In detail, the bearing, net tension and shear out stresses can be evaluated through the following equations:

$$\sigma_B = \frac{P}{D \cdot t_B} \quad \text{Eq. 1}$$

$$\sigma_{NT} = \frac{P}{(W - D) \cdot t} \quad \text{Eq. 2}$$

$$\tau_{SO} = \frac{P}{2 \cdot E \cdot t} \quad \text{Eq. 3}$$

It is worth noting that, in a particular geometrical configuration, a given failure mode happens if the failure mode stress reaches the limit strength for the considered failure mechanism. At the same time, the stress of the other failure modes remains lower than their limit strengths. A mixed mode happens when the stresses of two failure mechanisms reach nearby their limit at the same time.

To deeper understand the mechanical behaviour of the pin-loaded glass reinforced composite laminates, the evolution of the mechanical resistance and stress-displacement curves of these laminates was studied both at varying edge distance E (keeping constant W and D) and at varying the hole diameter D (keeping constant E and W).

Since the bearing failure mode is the preferred one by the designers in order to achieve the laminate full strength thus avoiding sudden and catastrophic failures, a correct prediction of this fracture mode despite the other competing ones (i.e., shear out, net tension or cleavage modes) is a desirable condition in design and optimization of mechanical joint performances. As widely done in literature [18,30–33], the static bearing strength was considered as the key comparative parameter to improve the mechanical knowledge of the joints as function of their geometrical configuration, thus indicating an effective approach for optimizing the mechanical performance of fastened joints designed for high bearing resistance [34,35]. For this reason, in the following paragraphs the joints resistance was evaluated by using equation 1, regardless of the failure mechanism experimentally occurred.

3.1 Effect of edge distance E

The bearing maximum stress of pin-loaded composites with 15 mm width, was shown as function of edge distance E, at varying also the hole diameter D (Figure 2).

Regardless the hole diameter, two different trends can be observed: i.e., for low edge distances the bearing stress increases proportionality with E, afterward it reaches a plateau. It is important to state that the samples with small hole diameter (i.e., 4 mm and 6 mm) experienced a transition in the failure mode from shear out to bearing by increasing the edge distance E. On the other hand, no bearing failures were observed for pin-loaded laminates with hole diameter equal to 8 and 10 mm: the failure mode changes from shear out (i.e., for low edge distance) to net tension (i.e., for high edge distance). Moreover, these last samples failed through a mixed mode (i.e., cleavage) for intermediate distance between the hole and the laminate free edge. By observing the graph, it is evident that the plateau values of the bearing stress increase by decreasing hole diameter. These different values can be explained taking into account the different failure modes occurred. By

analysing the bearing stress trend for samples with 4 mm hole diameter, at increasing edge distance a quite linear trend (high sensitive to edge distance) can be identified. In this region, the edge distance is very low and the shear out fracture mechanism is dominating. Thus induces a premature failure of the sample at very low applied load. The observed low bearing stress indicates the not effective mechanical stability of this joint geometry. However, at larger edge distance a different linear relationship between edge distance and bearing stress was observed. A plateau at high bearing stress level is reached (i.e., about 220 MPa). These samples evidenced bearing failure mechanism. Decreasing the hole diameter a bilinear trend of bearing stress evolution at increasing edge distance is still identifiable even if the plateau bearing stress at large edge distance progressively decreases. This effect could be due a progressive transition from bearing fracture mechanism (i.e., for samples with 4-6 mm hole diameter) to net tension one (i.e., for samples with 8-10 mm hole diameter).

In particular, the plateau bearing stress at high edge distances for pin-loaded laminates with 6 mm hole diameter (i.e., about 195 MPa) was found to be 11% lower than those having smaller hole (i.e., D = 4 mm), although both batches failed through the preferred bearing mode. Analogous consideration are reported in the literature [10,19] showing the progressive decrease of the ultimate bearing stress at increasing the hole diameter of the joint. This could be justified since bearing strength depends only on the maximum contact pressure applied on the contact [10] that decreases at increasing pin diameter. These considerations could justify the lower plateau bearing failure stress observed for samples with D=6 mm.

Since the samples having great hole (D=8 mm and D=10 mm) did not experience bearing failures, the bearing stresses evaluated in the plateau region is lower than the critical bearing limit stress. Even at very high edge distance, the failure mechanism of the pin-loaded composites with 10 mm hole diameter is dominated by a premature and catastrophic failure mechanism (i.e., net tension) thus inducing bearing stresses (about 90 MPa) consistently lower than the bearing critical limit of

the glass composite laminate. Furthermore, the plateau bearing stress reached by the samples with 8 mm hole diameter at high edge distances was found to be much higher than that of the pin-loaded composites with 10 mm hole diameter (i.e., 160 MPa vs 90 MPa). In fact, their failure mode can be indicated as a mixed mode identifiable as a threshold region between net tension and bearing failure mechanism.

Figure 3 shows a simplified scheme regarding the fracture mechanisms occurring by varying the geometrical properties of the joint. For any dimeter size, low values of E imply the damage evolution of the joint by shear out mechanism. On the other hand, two fracture mechanisms take place at very high E values: bearing mode and net tension mode for low and high diameter size, respectively. Finally, a short cleavage region was found as a transition between shear out and net tension fracture.

Figure 4 shows fracture images by shear out, net tension and bearing mode for three reference glass composite samples.

To better understand the different mechanical behaviour of the pin-loaded laminates at varying the geometrical configuration, the load-displacement curves of pin-loaded laminates with hole dimeter equal to 4 mm and 8 mm were shown in Figure 5.

First, it is important to note that the bearing stress-displacement curves of the pin-loaded laminates show an initial linear trend with slop quite constant; whatever it is their geometrical configuration. In both cases (i.e., hole diameter equal to 4 mm or 8 mm), samples characterized by the hole near to the laminate free edge (i.e., low edge distance) experienced premature and catastrophic fractures at low displacement and stress values, since they failed through brittle and sudden shear out mechanism. Samples with 4 mm hole diameter showed better mechanical stability by increasing edge distance, since bearing becomes the predominant failure mechanism. It is evident that if bearing failure of laminates is achieved by adequately choosing their geometrical configuration, they will possess great bearing capacity, thus carrying higher stresses before the final failure. This is

justified since bearing is the only progressive failure mode making it the preferred one in joining design in order to avoid catastrophic fractures through shear out, net tension or cleavage [4]

As already stated, shear out is the predominant failure mode for low hole to free edge distance, regardless the hole diameter D. It is worth noting that samples with 8 mm hole diameter show quite similar load-displacement curves, regardless of E values because, just catastrophic mechanisms happens (i.e., shear out, cleavage and net tension). For this reason, the maximum bearing stress carried by pin-loaded laminates with 8 mm hole diameter is lower than that of the laminates with lower hole diameter (i.e., about 170 vs 230 MPa).

Furthermore, despite regardless the edge distance E just catastrophic mechanisms happen, it is worth noting that this geometrical parameter influences the failure deformation of the samples. More in detail, when the hole is close to the laminate free edge (i.e., low edge distance E), the pin-hole connection characterized by shear out fracture evidenced an acceptable damage tolerance before its fracture: i.e., a large displacement before the final failure is evident for these samples. This deformation capability can be explained taking into account the elastic deformation of the laminate region rear the hole up to sample failure. On the other hand, an increase of the shear resistant cross section occurs at increasing laminate free edge distance E. Thus favours cleavage and net tension failures, for intermediate and high values of the edge distance E, respectively. In particular, when net tension becomes the predominant mechanism (i.e., for high edge distance) cracks perpendicularly to the applied load direction rapidly propagated at very low displacement values, thus leading to very low damage tolerance of the samples, due to the very brittle nature of the net tension mode. Finally, when cleavage mechanisms occurred, the pin- loaded laminates showed intermediate failure elongation in comparison to the previous cases: this is justified since cleavage can be considered as a mixed failure between the shear out and net tension

3.2 Effect of hole diameter D

Further information about the mechanical behaviour of pin-loaded glass reinforced laminates can be extrapolated by considering the influence of the hole diameter D on the bearing stress-displacement curves of samples with identical width and edge distance. Figure 6a shows the evolution of the stress-displacement curves for laminates with edge distance equal to 12 mm (with constant width W=15). For high hole diameter (i.e., 8mm), the tensile cross-section of the specimen is particularly small so that stimulates a premature and sudden failure through net tension. In this case, a stress concentration takes place at the pin-hole edge (i.e., the maximum stress decrease rapidly moving from the hole toward the sample edge). For this reason, the applied stress reaches easily the net tension critical strength of the laminate thus favouring the propagation of cracks perpendicularly to the loading direction from the hole edge toward the lateral laminate edges.

By decreasing the hole diameter, the tensile section of the specimen increases leading to damaging by compressive collapse in the pin/hole contact surface area, typical of bearing failure mode. This progressive and gradual collapse of the pin/hole boundary area is strictly related to the combination of delamination and fiber buckling phenomena [29]. The mechanism interaction implies a higher absorbed energy up to failure experienced by the pin-loaded laminates failed through bearing mode than those through net tension one: i.e., samples characterized by bearing fracture evidenced a good damage tolerance before the fracture of the material, thus improving the joint safety.

Furthermore, it is possible to note the samples stiffness (i.e., proportional to the stress- displacement curves slope) increases with decreasing the hole diameter as already reported in the literature [36], i.e., when the failure mode changes from net tension to bearing. The bearing stress-displacement curve for samples with edge distance equal to 9 mm, was shown as function of the hole diameter in Figure 6b. Similarly to the previous case, the predominant failure mechanism for small hole diameter (i.e., 4 and 6 mm) is the preferred bearing one. This means that the hole boundaries are far enough to the laminate edges to avoid catastrophic and premature failures such as net tension or

shear out, thus allowing to reach the laminate full strength. By increasing the hole diameter to 8 mm, a transition in the failure mode from bearing to cleavage can be observed for this samples. Unlike the pin-loaded laminates characterized by 12 mm edge distance, these last did not experience pure net tension failures at increasing the hole diameter but the mixed mechanism cleavage. This means that the in-plane shear stress plays an important role (i.e., together with the tensile stresses) in the failure of these laminates due to the position of the hole closer to the laminate free edge.

3.3 3D Failure maps

From the previous considerations, it was indicated that the joint geometry has a significant effect on the mechanical behavior of the composite joint having a key role both in the failure mechanism and on the resistance limit. In order to better understand how the different geometric parameters affect the mechanical strength capacity, Figure 7a shows the mesh surface plot of the bearing stress (calculated according to equation 1) at varying E/D and W/D geometrical ratios (in the range 0.5-4.5 and 1.0-5.0, respectively).

In the graph, line 1 highlights the effect of the variation of W/D ratio for wide joints (E/D = 2.4). Bearing strength increases monotonously until a critical W/D value is reached beyond which the stress remains quite constant [18]. The critical W/D ratio indicates the transition from net tension to bearing fracture. Similar considerations can be drawn by evaluating the effect of a wide-range E/D variation (W/D = 4.0, line 2). A threshold value of E/D is identifiable in correspondence of which stable mechanical performances of the joint can be observed. At large E/D values, the bearing mode is the dominating failure mechanism. Furthermore, the dotted line 2’ highlights the effect of the variation of E/D for medium low W/D ratio (W/D about 2.0). Line 2’ have a quite similar trend of line 2 although a different maximum value of bearing stress at high E/D ratio can be identified. This difference can be related considering that line 2 stress evolution is related to a transition from shear

out to bearing failure for low E/D and high E/D joint geometry, respectively. On the other hand, stress evolution evidenced in line 2' highlights a transition from shear out to net tension failure mechanism. Analyzing the mesh surface plot, a schemed failure map at varying joint geometry can be obtained in Figure 7b. The stress plateau clearly identifiable in the top right side of the plot identifies the bearing failure mechanism region. The average bearing strength in this region is about 220 MPa. For low E/D and high W/D values, the favored fracture mechanism is shear out mode. Conversely, for low W/D and high E/D values, fracture for net-tension is prevalent. Premature joint fractures for shear out and net tension imply a drastic drop in the bearing stress up to 150 MPa and 90 MPa for shear out and net tension failures, respectively.

As already stated, the ductile nature of bearing makes it the preferred failure mode among the other ones (i.e., shear out, cleavage and net tension) for joints designers [13,37]. For this reason, the static bearing strength is widely considered the key parameter in order to improve the knowledge of the mechanical behavior of the joints at varying their geometrical configuration [30,33].

In order to maintain a graphic order of the mesh surface plot in the failure map of Figure 7b it was not highlighted the cleavage fracture region, located in the boundary line between shear out and net tension fracture zones.

It is quite evident from Figure 7 that the weakest composite joint is obtained for very low E/D and W/D ratios. This means that, in this geometrical configuration, the hole is very close to the sample edge and at the same time it is large enough to drastically reduce the sample cross section thus favoring a premature and catastrophic failure (i.e., by a combined net tension and shear out mechanism) of the sample at very low stress level (i.e., 90 MPa). Only for high W/D (i.e., higher than about 2.4), and E/D (i.e., higher than about 1.6), ratios the strength increases to effective values. Above these threshold value the premature fracture of the sample for net tension or shear out is avoided and the progressive bearing failure mechanism is favored.

From a theoretical point of view, the evaluation of the bearing stress have physical meaning only when the pin-loaded laminates failed through bearing mode. This means that the bearing stress represents the real joint resistance just in the top right side of the plot (i.e., where bearing mode is the predominant one). Depending on the geometrical configurations for which net tension or shear out failures happen, it should be required to calculate their critical stresses (by using equations 2 and 3, respectively). In order to evidence which failure mode is the predominant for each geometrical configuration of the joint, it is possible to compare each component of the stress state to the material strength properties, thus calculating a failure index (FI) for each failure mechanism according to the maximum stress criterion. In particular:

$$FI_B = \frac{\sigma_B}{X_B} \quad \text{Eq. 1}$$

$$FI_{NT} = \frac{\sigma_{NT}}{X_{NT}} \quad \text{Eq. 2}$$

$$FI_{SO} = \frac{\sigma_{SO}}{X_{SO}} \quad \text{Eq. 3}$$

Where X_B, X_{NT} and X_{SO} are the bearing, net tension and shear out stress limits, respectively. These parameters were experimentally determined. Following this way, a failure mechanism can be forecasted when its specific FI has a value of 1 or above. A value between 0 and 1 will also provide an indication of how the sample with a specific geometrical configuration is close to a given failure mode.

Similarly, to the 3D mesh plot of the bearing stress, it is possible to draw a 3D plot of the failure indexes for bearing, net tension and shear out (Figure 8). For graphic convenience, fracture indexes greater than one have been indicated to be equal to 1. These graphs allow to clearly identify the region in which a given fracture mode is the predominant one (identified by the red zones).

3.4 Failure Map: experimental results versus theoretical model

The experimental results have clearly shown that the geometrical configuration of a pin-loaded laminate substrate influence the fracture mechanism of a mechanical joint thus greatly varying its resistance. In particular, variations of E/D and W/D ratio allow to change the failure mode from catastrophic and sudden one (i.e., shear out, net tension or cleavage) to progressive one (i.e., bearing). By adequately choosing of these geometrical parameters, it will be possible to design structural joints having high strength capability. By doing so, the progressive and gradual compressive collapse of composite laminate around the hole boundary will provide an effective warning before the final fracture of the mechanical joined composite structure.

The effect of the geometrical parameters on the failure modes can be easily highlighted by observing the 2D experimental failure map (Figure 9), built merely by placing the experimental results (i.e., the failure mechanism occurred at each combination of the geometrical parameters) in the plane E/D versus W/D ratios.

As noted above, premature fractures have been found for low deformation and/or displacement values. In particular, for net tension and shear out fracture conditions, the strain-displacement curve showed a sudden collapse indicating the catastrophic nature of the fracture mode. Both failure mechanisms cannot be considered reliable failure in engineering join design. On the other hand, fastened joints that exhibited bearing failure mechanism evidenced high stress level also at high deformation, confirming the progressive nature of this failure mode. This behaviour is related to the gradual compression collapse of the glass composite laminate near the hole just in contact with the pin. For geometrical joint configurations involving bearing fracture, the composite bolt joints exhibit greater damage resistance and provide an effective and valid alert condition that preserves the composite structure mechanically attached to an accidental crash. The bearing fracture becomes the predominant failure mechanism for high W/D and E/D ratios (point 1 in Figure 9). Following the dashed arrow from point 1 to point 2, indicating a reduction in the W/D ratio, maintaining a

constant E/D ratio (this is achievable making a larger diameter, but at a distance of the hole from the edge, E, constant) a transition from bearing to net tension failure mode can be observed at about W/D = 2.1. Increasing hole diameter D with constant W the cross section of the composite laminate in correspondence of the hole significantly is reduced thus inducing a higher stress concentration and consequently favoring the premature fracture of the sample for net tension. Afterward, following the dotted arrow that link point 2 to point 3, indicating a decrease of the E/D ratio maintaining a constant W/D ratio, a transition from net tension to shear out can be observed (the threshold value can be identified at E/D=1.6). Point 3 in Figure 9 identifies a region where shear out fracture occurred. In fact, decreasing E value, maintaining constant the other joint geometrical parameters (D and W), the distance of the hole from the free edge becomes very small. This geometrical configuration is characterised by a reduced shear cross section, thus stimulating a premature shear out fracture. However, a transition region at the boundary between net tension and shear out fracture mechanics are was observed, as a consequence of the mixed cleavage fracture onset [13]. Consequently, the cleavage failure mode could be indicated a combined fracture mechanism between net tension and shear out mode where neither of previous mechanisms is prevalent, thus inducing a mixed premature fracture mechanisms [18] [13].

From a theoretical point of view, fixing the joint geometry, a given failure mechanism takes place if the applied stress reaches its strength limit. For this reason, it need to just equalize the fracture load threshold for each failure mechanism (evaluated from equations 1-3) to obtain the following equations:

Transition Bearing/Net-tension	$\frac{W}{D} = X_B/X_{NT} + 1$	Eq. 7
Transition Bearing/Shear out	$\frac{E}{D} = 1/2 \cdot X_B/X_{SO}$	Eq. 8
Transition Shear-out/Net-tension	$\frac{W}{D} = 2 \cdot X_{SO}/X_{NT} \cdot e/d + 1$	Eq. 9

These equations determine three transition straight lines in the E/D–W/D plane, able to divide the failure plane into three zones each characterized by the corresponding fracture mode. In particular, it is possible to predict theoretically the fracture mechanisms regions by using in the equations 7-9 the experimental values of bearing, shear out and net tension stress limits (X_B, X_{NT} and X_{SO}) equal to 220, 150 and 90 MPa, respectively.

Figure 10 shows the theoretical failure regions. It is important to state that this theoretical model is not able to predict the cleavage area since the cleavage stress was not analytically evaluated. Nevertheless, for sake of clearness the presence of this mixed mechanism was also indicate across the shear out-net tension transition line.

Comparing Figures 8 and 9 the efficacy of the simplified theoretical model can be evidenced: i.e., the theoretical model provides a very good match with the experimental results, thus furnishing a clear and real subdivision of the W/D-E/D plane into net tension, shear out and bearing regions.

As already shown in our previous paper [18], the progressive and gradual bearing mechanism becomes the predominant one in the upper right corner, that represents the most interesting and desired design zone of the plot. This means that, in order to achieve the laminate full strength and guarantee a not catastrophic failure thus providing an effective warning before the final fracture of the mechanical joined structure, E/D and W/D ratios must be higher than about 1.6 and 2.1, respectively.

The comparison of these threshold limits with those obtained in our previous paper [18] (i.e., 2 and 3 for E/D and W/D, respectively), evidenced that a larger bearing zone has been found in the present paper. This is justified since, as widely known [27,33,38], the mechanical behaviour of pin-loaded composite laminates is strongly influence by the stacking sequence. In this concern, future research activities will be focused on how the presence of lignocellulosic woven fabrics (i.e., such

as jute or flax) instead of glass woven ones can modify the mechanical behaviour of pin-loaded hybrid laminates.

4 Conclusions

In this paper, the assessment of the bearing performances of fiberglass composite joints has been reported. In particular, single bolt joints tests were carried out at varying geometric parameters such as hole diameter D, composite width W and hole position from free edge of laminate, E.

The results highlighted that the joint configuration has a relevant influence on the mechanical stability and on joint failure mechanism. Maximum strength values were found for high values of E/D and W/D ratios with an average bearing stress of about 220 MPa. Conversely, low E/D or W/D values induced a significant reduction in mechanical performances due to premature joint fractures for shear out or net tension mechanisms, respectively. The minimum strength value, 90 MPa, was found for joints with E/D and W/D equal to 0.6 and 1.5, respectively.

Furthermore, a simplified theoretical failure map on E/D and W/D axes, was proposed in order to forecast in a simple way the mechanical behaviour of single bolt joints. The theoretical results showed a good matching with experimental one validating the proposed approach. In particular, the proposed simplified failure map highlighted that, in woven glass fibre composite laminates mechanically fastened joints should have, E/D and W/D ratios higher than 1.6 and 2.1 respectively in order to stimulate a progressive bearing failure mechanism.

Finally, another goal of the present paper was to accurately capture 3D shape information for the evaluation of the failure mechanisms by drawing a 3D plot (i.e., at varying E/D and W/D geometrical ratios) of the failure indexes (FI) evaluated for each failure mechanism according to the maximum stress criterion.

References

[1] N.G. Tsouvalis and V.A. Karatzas, *Appl. Compos. Mater.*, **18**, 149 (2011).

[2] K.N. Anyfantis and N.G. Tsouvalis, *Compos. Struct.*, **96**, 850 (2013).

[3] A. Valenza, V. Fiore and L. Fratini, *Int. J. Adv. Manuf. Technol.*, **53**, 593 (2011).

[4] V. Fiore, L. Calabrese, E. Proverbio, R. Passari and A. Valenza, *Compos. Part B Eng.*, **108**, 65 (2017).

[5] V. Fiore, F. Alagna, G. Di Bella and A. Valenza, *Compos. Part B Eng.*, **48**, 79 (2013).

[6] V. Fiore, F. Alagna, G. Galtieri, C. Borsellino, G. Di Bella and A. Valenza, *Compos. Part B Eng.*, **45**, 911 (2013).

[7] V. Fiore, L. Calabrese, E. Proverbio, G. Galtieri, T. Scalici, V.M. Lo Presti and A. Valenza, *J. Adhes. Sci. Technol.*, **30**, 2157 (2016).

[8] J. Zhang, F. Liu, L. Zhao, J. Zhi, L. Zhou and B. Fei, *J. Reinf. Plast. Compos.*, **34**, 388 (2015).

[9] J.L. York, D.W. Wilson and R.B. Pipes, *J. Reinf. Plast. Compos.*, **1**, 141 (1982).

[10] G. Catalanotti and P.P. Camanho, *Compos. Sci. Technol.*, **76**, 69 (2013).

[11] T.S. Lim and D.G. Lee, *Compos. Struct.*, **56**, 211 (2002).

[12] M.F. Wilhelm, U. Fuessel, T. Richter, M. Riemer and M. Foerster, *J. Compos. Mater.*, **49**, 981 (2015).

[13] L. Feo, G. Marra and A.S. Mosallam, *Compos. Struct.*, **94**, 3769 (2012).

[14] B. Okutan, Z. Aslan and R. Karakuzu, *Compos. Sci. Technol.*, **61**, 1491 (2001).

[15] F. Ascione, L. Feo and F. Maceri, *Compos. Part B Eng.*, **41**, 482 (2010).

[16] B. Vangrimde and R. Boukhili, *Compos. Part B Eng.*, **34**, 593 (2003).

[17] A. Aktas and M. Husnu Dirikolu, *Compos. Sci. Technol.*, **64**, 1605 (2004).

[18] A. Valenza, V. Fiore, C. Borsellino, L. Calabrese and G. Di Bella, *J. Compos. Mater.*, **41**, 951 (2007).

[19] G. Turvey, Failure of single-lap single-bolt tension joints in pultruded glass fibre reinforced plate, in: 6th Int. Conf. Compos. Constr. Eng., Rome (Italy), .

[20] M. Ozen and O. Sayman, *Compos. Part B Eng.*, **42**, 264 (2011).

[21] Z. Wang, S. Zhou, J. Zhang, X. Wu and L. Zhou, *Mater. Des.*, **37**, 582 (2012).

[22] P.J. Gray and C.T. McCarthy, *Compos. Sci. Technol.*, **71**, 1517 (2011).

[23] Y. Tang, Z. Zhou, S. Pan, J. Xiong and Y. Guo, *Mater. Des.*, **65**, 243 (2015).

[24] L. Zhao, T. Qin, J. Zhang, M. Shan and B. Fei, *J. Compos. Mater.*, **49**, 1667 (2015).

[25] J. Zhang, F. Liu, L. Zhao and B. Fei, *Compos. Struct.*, **108**, 129 (2014).

[26] P.P. Camanho and M. Lambert, *Compos. Sci. Technol.*, **66**, 3004 (2006).

[27] P.P. Camanho and F.L. Matthews, *Compos. Part A Appl. Sci. Manuf.*, **28**, 529 (1997).

[28] S.D. Thoppul, J. Finegan and R.F. Gibson, *Compos. Sci. Technol.*, **69**, 301 (2009).

[29] T. Yýlmaz and T. Sýnmazçelik, *Mater. Des.*, **28**, 520 (2007).

[30] G. Caprino, G. Giorleo, L. Nele and A. Squillace, *Compos. - Part A Appl. Sci. Manuf.*, **33**, 779 (2002).

[31] U.A. Khashaba, H.E.M. Sallam, A.E. Al-Shorbagy and M.A. Seif, *Compos. Struct.*, **73**, 310 (2006).

[32] H.J. Park, *Compos. Struct.*, **53**, 213 (2001).

[33] G. Kretsis and F.L. Matthews, *Composites*, **16**, 92 (1985).

[34] J. Ekh, J. Schön and D. Zenkert, *Compos. Struct.*, **105**, 35 (2013).

[35] A. Crosky, D. Kelly, R. Li, X. Legrand, N. Huong and R. Ujjin, *Compos. Struct.*, **76**, 260 (2006).

[36] G.J. Turvey, *Compos. Struct.*, **42**, 341 (1998).

[37] Á. Olmedo and C. Santiuste, *Compos. Struct.*, **94**, 2110 (2012).

[38] C.N. Rosner and S.H. Rizkalla, *J. Mater. Civ. Eng.*, **7**, 223 (1995).

Table Captions

Table 1. Details of geometric parameters of composite samples used for bearing tests

Figure Captions

Figure 1. a) Geometry of composite samples and b) Scheme of the set-up of the bearing test on composite bolted joint

Figure 2. Bearing stress at increasing edge distance E

Figure 3. Scheme of failure mechanisms evolution in bearing stress vs edge distance E plot

Figure 4. Images of a) shear out fracture on G_4_4_15 b) net tension fracture on G_8_8_15 c) bearing fracture on G_6_15_15

Figure 5. Bearing stress-displacement curves at varying edge distance for samples with a) 4 mm and b) 8 mm hole diameter

Figure 6. Load-displacement curves at varying hole diameter for samples with (a) 9 mm edge distance and (b) 12 mm edge distance

Figure 7. a) Mesh 3D surface plot and b) failure mechanisms map on mesh 3D surface plot of bearing stress at varying E/D and W/D parameters

Figure 8. Mesh 3D surface plot of a) bearing b) net tension c) shear out failure index at varying E/D and W/D parameters

Figure 9. Failure mechanisms in E/D versus W/D plot

Figure 10. Theoretical failure map of for flax/epoxy composite joints

Table 1. Details of geometric parameters of composite samples used for bearing tests

	Hole diameter D	Edge E	Width W
CODE	[mm]	[mm]	[mm]
G_4_4_15	4	4	15
G_4_5_15	4	5	15
G_4_6_15	4	6	15
G_4_8_15	4	8	15
G_4_9_15	4	9	15
G_4_10_15	4	10	15
G_4_12_15	4	12	15
G_6_5_15	6	5	15
G_6_6_15	6	6	15
G_6_7_15	6	7	15
G_6_9_16	6	9	16
G_6_12_15	6	12	15
G_6_15_15	6	15	15
G_6_6_18	6	6	18
G_6_12_19	6	12	19
G_6_15_18	6	15	18
G_8_6_15	8	6	15
G_8_8_15	8	8	15
G_8_9_15	8	9	15
G_8_10_15	8	10	15
G_8_12_15	8	12	15
G_8_14_15	8	14	15
G_8_16_15	8	16	15
G_8_19_15	8	19	15
G_8_14_17	8	14	17
G_8_19_18	8	19	18
G_10_6_15	10	6	15
G_10_9_15	10	9	15
G_10_10_15	10	10	15
G_10_13_15	10	13	15
G_10_15_17	10	15	17

G_10_18_15	10	18	15

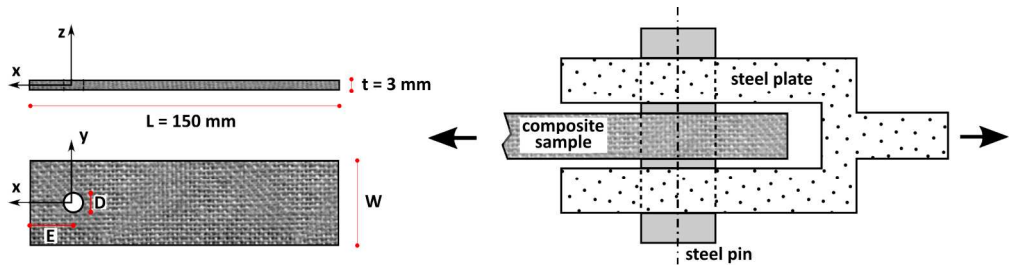

Figure 1. a) Geometry of composite samples and b) Scheme of the set-up of the bearing test on composite bolted joint

189x48mm (300 x 300 DPI)

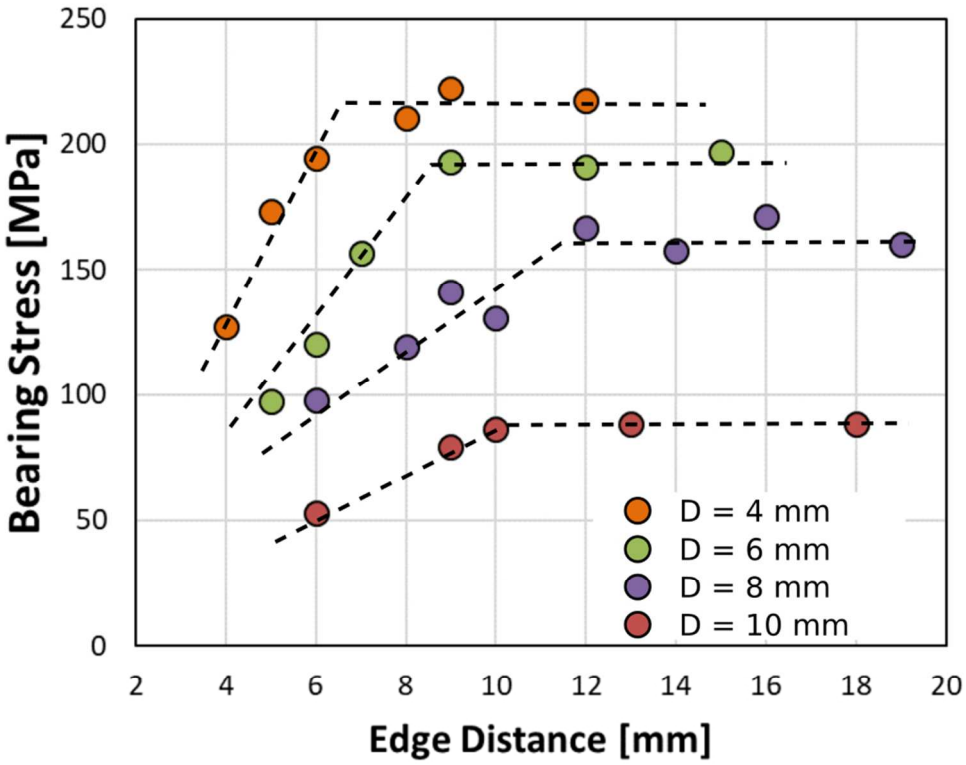

Figure 2. Bearing stress at increasing edge distance E

90x70mm (300 x 300 DPI)

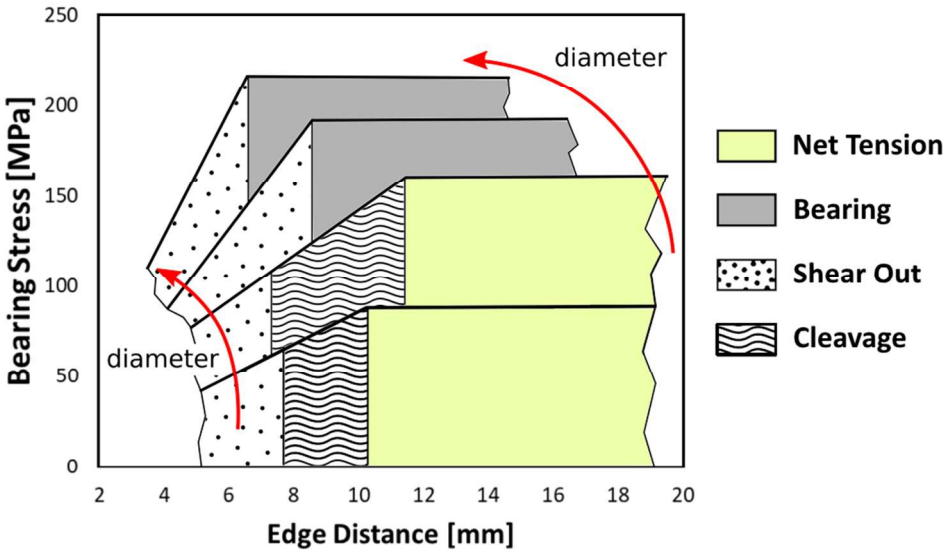

Figure 3. Scheme of failure mechanisms evolution in bearing stress vs edge distance E plot

94x54mm (300 x 300 DPI)

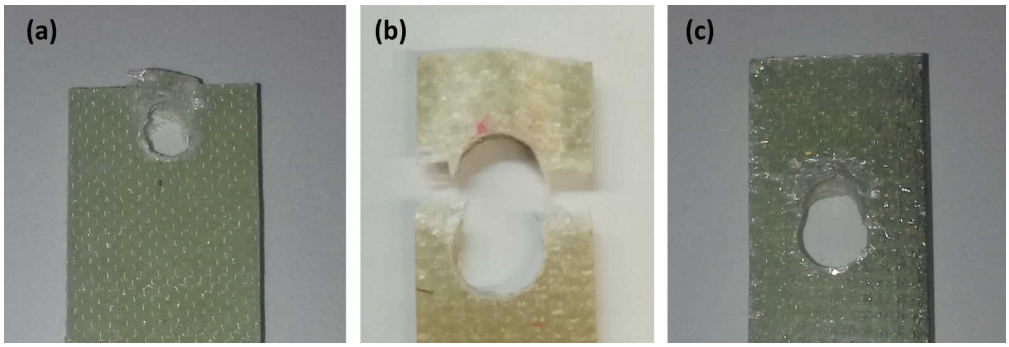

Figure 4. Images of a) shear out fracture on G_4_4_15 b) net tension fracture on G_8_8_15 c) bearing fracture on G_6_15_15

189x63mm (300 x 300 DPI)

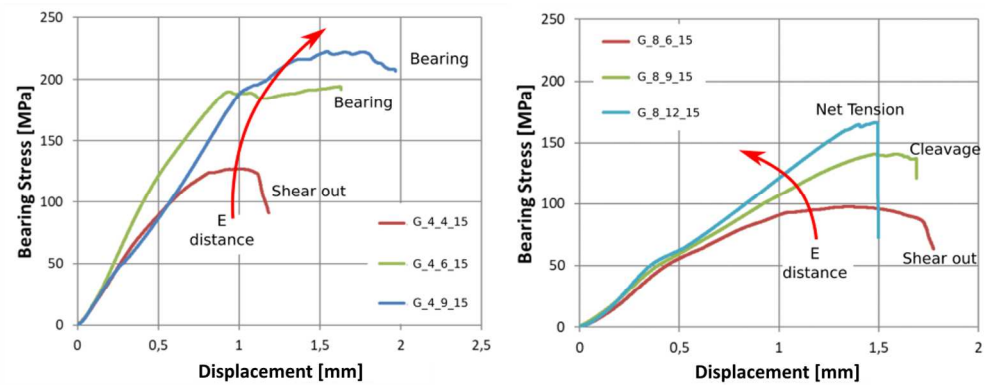

Figure 5. Bearing stress-displacement curves at varying edge distance for samples with a) 4 mm and b) 8 mm hole diameter

134x51mm (300 x 300 DPI)

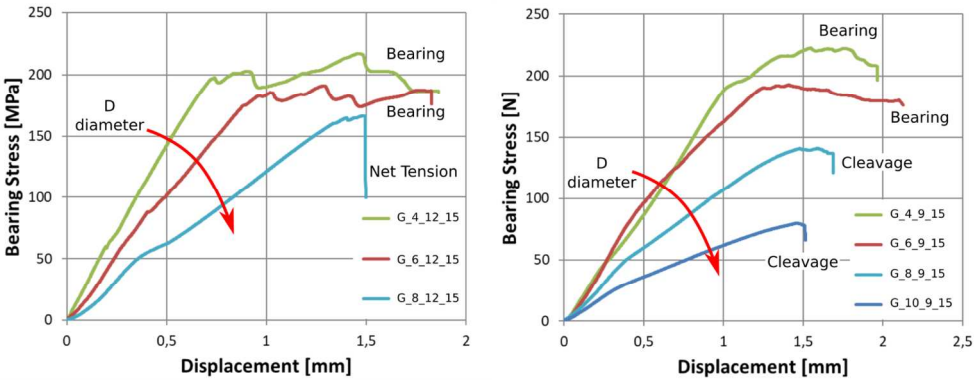

Figure 6. Load-displacement curves at varying hole diameter for samples with (a) 9 mm edge distance and (b) 12 mm edge distance

134x51mm (300 x 300 DPI)

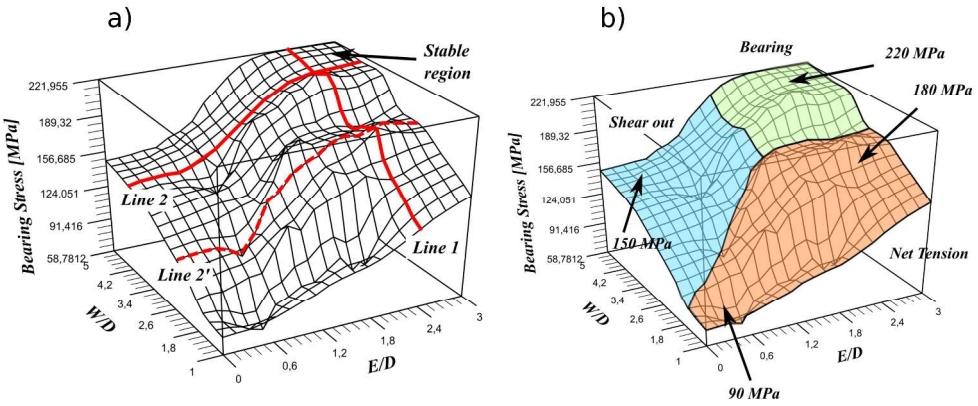

Figure 7. a) Mesh 3D surface plot and b) failure mechanisms map on mesh 3D surface plot of bearing stress at varying E/D and W/D parameters

2696x1106mm (72 x 72 DPI)

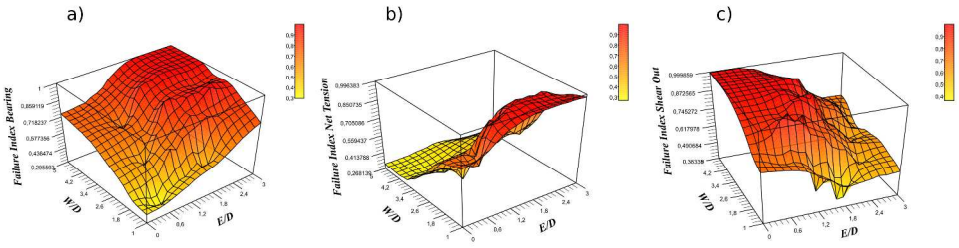

Figure 8. Mesh 3D surface plot of a) bearing b) net tension c) shear out failure index at varying E/D and W/D parameters

2653x708mm (72 x 72 DPI)

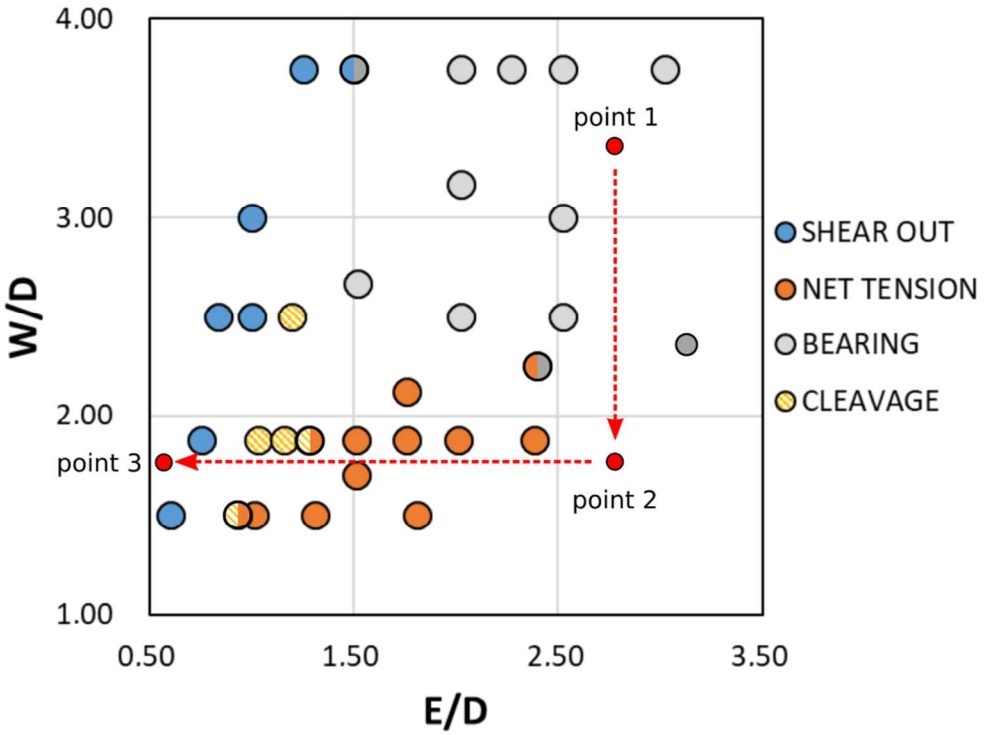

Figure 9. Failure mechanisms in E/D versus W/D plot

90x66mm (300 x 300 DPI)

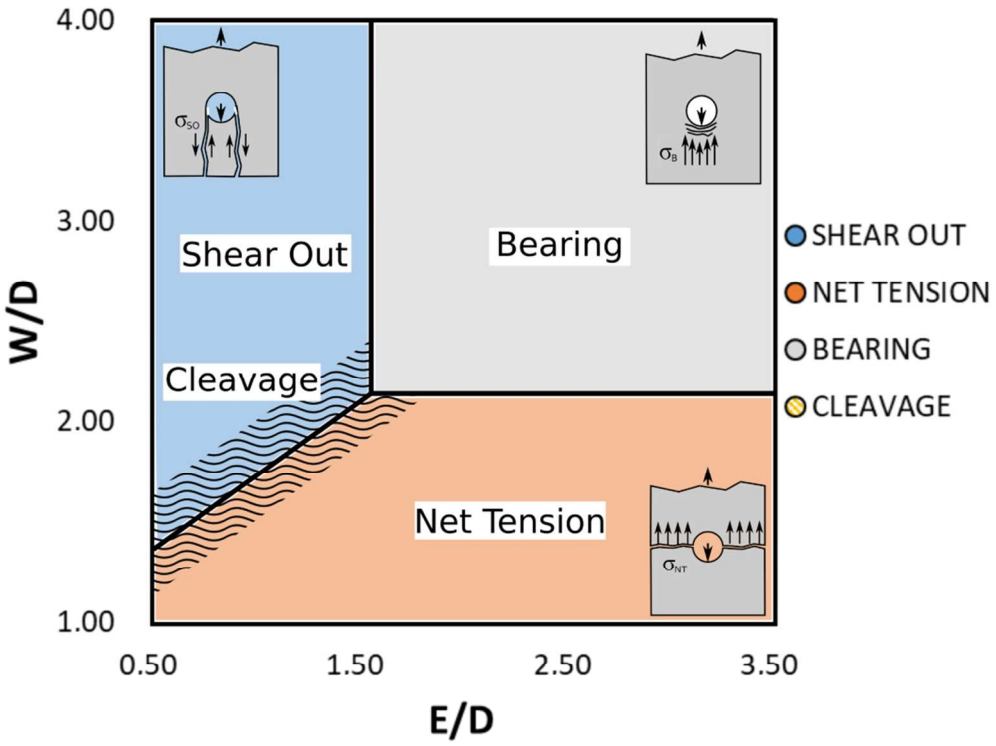

Figure 10. Theoretical failure map of for flax/epoxy composite joints

90x68mm (300 x 300 DPI)